Constructing magnetic polyaniline/metal hybrid nanostructures using polyaniline/Fe$_3$O$_4$ composite hollow spheres as supports

Lirong Kong, Xiaofeng Lu, E Jin, Shan Jiang, Xiujie Bian, Wanjin Zhang *, Ce Wang *

Alan G. MacDiarmid Institute, Jilin University, Changchun 130012, PR China

ABSTRACT

Polyaniline (PANI)/Fe$_3$O$_4$ composite hollow spheres have been successfully synthesized in one step using sulfonated polystyrene (PS) spheres as templates. The magnetic PANI hollow spheres were used as supports for noble metal nanoparticles (NPs) such as Au and Pd. The morphology, composition and magnetic properties of the resulting products were characterized by scanning electron microscopy (SEM), transmission electron microscopy (TEM), X-ray diffraction (XRD), Fourier transform infrared (FTIR) spectroscopy, inductively coupled plasma (ICP) atomic spectra and vibrating sample magnetometer. The catalytic activity of magnetic PANI/Au composite shells on the oxidation of dopamine was investigated by cyclic voltammetry. The obtained results provide our product with a practical application for the detection of dopamine. On the other hand, the catalytic activity of magnetic PANI/Pd composite shells on the reduction of 4-nitroaniline was investigated by spectroscopic methods and compared with Pd/C catalyst which was already widely used in industrial production.

© 2009 Elsevier Inc. All rights reserved.

1. Introduction

Polymer capsules and hollow spheres have increasingly attracted interest because of their large surface area and potential applications in catalysis, controlled delivery, artificial cells, light fillers, low dielectric constant materials, acoustic insulation, and photonic crystals [1]. These particles have been synthesized by using mono-dispersed particles and their arrays as templates. Recent years, there has been increased interest in the fabrication of composite hollow spheres using conducting polymer hollow spheres as supports for metal nanoparticles (NPs) or other catalysts [2–7]. Polyaniline (PANI) is one of the most important conducting polymers because of its high conductivity, ease of preparation, good environmental stability, mechanical flexibility and low cost. When PANI is used as support, it can be also acted as reducing agent and stabilizer. These advantages translate into easy and reproducible syntheses that make metal NPs supported by PANI [8,9] promising candidates for organic catalysis.

On the other hand, magnetic iron oxide NPs, e.g., Fe$_3$O$_4$ NPs, have also received considerable interest because of their broad range of possible applications in magnetic memories, electronics, catalysis, and vitro/vivo applications. The latter includes aspects such as magnetic bioseparation [10–12], biological labeling and diagnostics, enhancement of contrast agents for magnetic resonance imaging, hyperthermia of tumors, and drug-carrier design

[13–15]. Thereby, magnetic nanocomposites have been the focus of many researchers in recent years. In catalysis, these nanocomposites provide not only large surface areas for high loading of catalysts but also the ability to be easily separated from reaction mixture by means of the using of an external magnetic field.

Based on the unique properties of PANI hollow spheres and Fe$_3$O$_4$ NPs, we designed the synthesis of PANI/Fe$_3$O$_4$ NPs composite hollow spheres and used them as supports for noble metal NPs. As a result, the obtained magnetic PANI/metal hybrid nanostructures exhibit enhanced catalytic activities and can be easily separated from reaction mixture by using an NdFeB permanent magnet.

2. Experimental procedure

2.1. Materials

Aniline and styrene monomer was distilled under reduced pressure and stored below 0 °C before use. Phosphate-buffered saline (PBS, 50 mM KH$_2$PO$_4$+50 mM Na$_2$HPO$_4$, pH 7.0) was used as supporting electrolytes. Other reagents were analytical grade and used without further purification including FeCl$_3 \cdot$6H$_2$O, FeCl$_2 \cdot$4H$_2$O, NH$_3 \cdot$H$_2$O, acetone, succinic anhydride, diethyl ether, CH$_2$Cl$_2$, ammonium peroxydisulfate (APS), sulfuric acid (H$_2$SO$_4$), potassium persulfate (K$_2$S$_2$O$_8$, KPS), NaBH$_4$, PdCl$_2$, tetrahydrofuran (THF), trisodium citrate, HAuCl$_4 \cdot$4H$_2$O Pd/C (10%) catalyst, *p*-nitroanilinum and ethanol (99.7%). Aniline dimer-COOH was

synthesized by our group [16]. Dopamine (DA) was obtained from Fluka. The water used in the experiments was distilled water.

2.2. Synthesis of decorated Fe_3O_4 NPs

Decorated Fe_3O_4 NPs were prepared based on our previous report [17]. $FeCl_2 \cdot 4H_2O$ (0.86 g) and $FeCl_3 \cdot 6H_2O$ (2.35 g) were dissolved under N_2 in deaerated Milli-Q water (20 mL) under vigorous stirring. As the solution was heated to 60 °C, $NH_3 \cdot H_2O$ (28% (w/w), 5 mL) was added, quickly followed by addition of a solution of aniline dimer-COOH (200 mg) in 2 mL of acetone. The reaction was allowed to proceed for 1 h at 80 °C with constant and vigorous stirring to produce a stable, water-based suspension. The reaction mixture was then cooled slowly to room temperature. The suspension was washed sequentially with acetone and ethanol.

2.3. Preparation of polystyrene (PS) and sulfonated PS spheres

Mono-dispersed PS spheres (340 nm in diameter) were prepared according to the following procedure [2]. Styrene monomer (10 g) was added to 140 g of distilled water under stirring for 10 min at 70 °C in a nitrogen atmosphere. An aqueous solution of initiator (10 g containing 0.23 g of potassium persulfate) was added, and the reaction was held for 24 h. Finally, the emulsion was naturally cooled to ambient temperature, and the mono-dispersed PS colloid was obtained. The above PS colloid was centrifuged (9000 rpm, 10 min) and washed with distilled water. The wet PS spheres were dispersed in 30 mL of concentrated sulfuric acid. The sulfonation reaction was allowed to take place at 40 °C for 4 h. The product was centrifuged and washed with distilled water; wet sulfonated PS spheres were then obtained.

2.4. Preparation of PANI hollow spheres containing Fe_3O_4 NPs in their matrix

Wet sulfonated PS spheres (0.8 g) were directly dispersed in 20 mL water. Decorated Fe_3O_4 NPs (0.16 g) and aniline monomer (0.2 g) were added to the mixture under stirring. Stirring was continued for 10 h. An aqueous solution of APS (5 mL, 1:1 molar ratio of APS to aniline) was added, and the reaction was allowed to proceed for 12 h. After the reaction, the solution was centrifuged, and the precipitate was washed with distilled water and ethanol several times. The final product was dried in vacuum at 50 °C for 12 h. The PANI/Fe_3O_4 NPs composite hollow spheres were prepared by dissolving PS cores from the PANI/Fe_3O_4 NPs-coated PS spheres in THF.

2.5. Preparation of PANI/Fe_3O_4 NPs/Au composite hollow spheres

The Au colloid was prepared according to the reported method by boiling $HAuCl_4$ aqueous solution with trisodium citrate [18]. The average diameter of the prepared Au NPs is about 12 nm. PANI/Fe_3O_4 NPs hollow spheres were added to the Au colloid (1.0 mg/mL) under stirring. The reaction was allowed to proceed for 12 h, and the resultant product was centrifuged and dried. Au NPs could be adsorbed on the surface of PANI, leading to the formation of PANI/Fe_3O_4 NPs/Au composite hollow spheres. The amount of Au NPs adsorbed on the PANI surface could be controlled by adjusting the concentration of PANI/Fe_3O_4 NPs in the Au colloid [2].

2.6. Preparation of PANI/Fe_3O_4 NPs/Pd composite hollow spheres

Wet sulfonated PS spheres (0.1 g) were directly dispersed in water (20 mL). $PdCl_2$ (0.05 g) was added to the above polymer solution under stirring. Then the solution was heated to 60 °C and kept stirring for 1 h. After that, 0.05 g $NaBH_4$ was dissolved in distilled water (2 mL) and added to the above mixture drop by drop. The reduction process of Pd^{2+} ions lasted for about 1 h. The composite was filtered, washed with water and dried at 50 °C for 12 h. Then we repeated the preparation process of PANI/Fe_3O_4 NPs composite hollow spheres using Pd/PS spheres instead of PS/sulfonated PS spheres. Then the PANI/Fe_3O_4 NPs/Pd composite hollow spheres were obtained.

2.7. Characterization

Scanning electron microscopy (SEM) measurements were performed on a SHIMADZU SSX-550 microscope. Transmission electron microscopy (TEM) experiments were performed on a Hitachi 8100 electron microscope (Tokyo, Japan) with an acceleration voltage of 200 kV. Fourier transform infrared (FTIR) spectra of KBr powder-pressed pellets were recorded on a BRUKER VECTOR22 Spectrometer. X-ray diffraction (XRD) patterns were obtained with a Siemens D5005 diffractometer using $CuK\alpha$ radiation. ICP analysis was performed on Emission Spectrometer Plasma 1000 (PERKIN ELMER). During the process, the solid product was calcined under O_2 atmosphere, then treated with concentrate nitric acid and at last diluted to 50 mL by distilled water. The concentrations of the metal ions can be determined by the machine. The room temperature magnetization in the applied magnetic field was performed by model JDM-13 vibrating sample magnetometer. CHI660B Electrochemical Workstation (Shanghai CH Instruments, China) was used for electrochemical measurements. All electrochemical measurements were performed using a three-electrode configuration, consisting of the GC working electrode, an saturated calomel electrode (SCE) reference electrode and a platinum wire counter electrode, respectively. The UV spectra of 4-nitroaniline were measured by a Shimadzu UV-2501 PC Spectrometer.

2.8. Catalytic activity measurements

PANI/Fe_3O_4 NPs/Au composite hollow spheres have been decorated on the glassy carbon electrode (GCE) for the detection of DA. The decorated GCE was immersed in PBS solution containing different concentrations of dopamine and the cyclic voltammogram (CV) plots were recorded from −0.1 to 0.5 V with a scan rate of 100 mV/s.

As a model reaction, we compared catalytic activity of the final product with Pd/C catalyst on the reduction of 4-nitroanilinum by $NaBH_4$. In a typical run, 0.2 mL catalyst aqueous solution with the Pd concentration of 0.2 mg/mL was added to a mixture of 1.4 mL 4-nitroaniline (0.4 mM) and 1.4 mL $NaBH_4$ (30 mM). The molar ratio of Pd to 4-nitroanilinum was kept at 1:3 during the reaction. According to the ICP result, the weight percentage of Pd in our product is 37.05% while in Pd/C is 10%. As a result, we tuned the concentrations of their dispersion to keep the concentration of Pd used as catalyst constant. The absorption spectra of the reaction solution were recorded at different time after the addition of the catalyst.

3. Results and discussion

3.1. Characterization

The process for the formation of the PANI/Fe_3O_4 composite hollow spheres is shown in Scheme 1. First, aniline and decorated
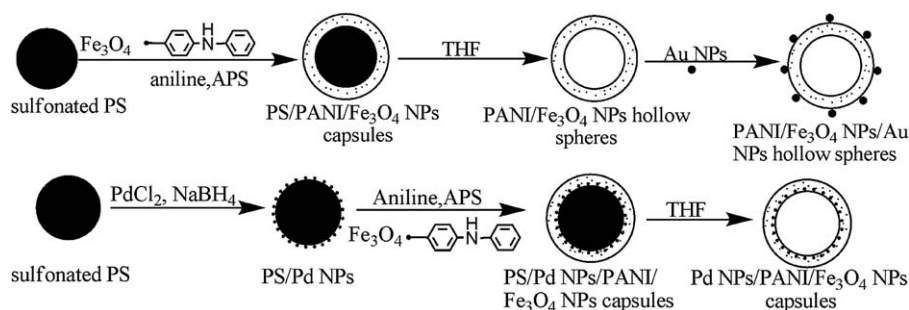
Scheme 1. Simplified schematic representations of the fabrication of PANI/Fe$_3$O$_4$, PANI/Fe$_3$O$_4$/Au and PANI/Fe$_3$O$_4$/Pd hollow spheres.

Fe$_3$O$_4$ NPs were absorbed to sulfonated PS spheres simultaneously. After the adding of oxidant, the in-situ polymerization of aniline happened and aniline dimmer decorated Fe$_3$O$_4$ NPs were fixed in the PANI matrix during the co-polymerization. PANI/Fe$_3$O$_4$ hollow spheres were obtained by dissolving PS cores with THF. When the polycationic PANI/Fe$_3$O$_4$ hollow spheres were introduced into the Au colloid, Au-decorated PANI/Fe$_3$O$_4$ hollow spheres were formed by an electrostatic effect because the surface of citrate stabilized Au NPs was electronegative. PANI/Fe$_3$O$_4$/Pd hollow spheres can be prepared by first decorating PS spheres with Pd NPs on their surface, followed by the in-situ polymerization of aniline and the dissolution of PS cores. From their SEM images (Fig. 1), we can find that the surface of hollow PANI spheres decorated with Fe$_3$O$_4$ NPs or metal NPs was rough while that of pure PANI hollow spheres was smooth. The Fe$_3$O$_4$ NPs could be clearly seen in the TEM image of PANI/Fe$_3$O$_4$ hollow spheres (Fig. 1d) with a diameter of about 5 nm. In the TEM image of PANI/Fe$_3$O$_4$/Pd hollow spheres, Pd NPs also have a diameter of about 5 nm while in the TEM image of PANI/Fe$_3$O$_4$/Au hollow spheres, Au NPs have a diameter of 13 nm. What is more, we can also find from the TEM images that Fe$_3$O$_4$, Pd and Au NPs are almost mono-dispersed. In order to determine the weight percentages of the inorganic NPs in the final composites, we analyzed them using ICP and found that the weight percentages in PANI/Fe$_3$O$_4$/Pd hollow spheres are: Fe$_3$O$_4$, 45.76% and Pd, 37.05% while the weight percentages in PANI/Fe$_3$O$_4$/Au hollow spheres are: Fe$_3$O$_4$, 42.29% and Au, 2.45%.

The existence of PANI in PANI/Fe$_3$O$_4$, PANI/Fe$_3$O$_4$/Au and PANI/Fe$_3$O$_4$/Pd hollow spheres was confirmed by FTIR spectra (Fig. 2). As shown, the characteristic peaks of PANI [19,20] at around 3428 (N–H stretching), 1571, 1492 (C = C stretching deformation of quinoid and benzenoid ring, respectively), 1300 (C–N stretching of secondary aromatic amine), 1123 and 832 cm^{-1} (out-of plane deformation of C–H in the 1, 4-disubtituted benzene ring) can be found in the spectra of the three PANI/Fe$_3$O$_4$ composites, indicating the presence of PANI in such three kinds of composites.

The XRD patterns of PANI, PANI/Fe$_3$O$_4$ and metal NPs/PANI/Fe$_3$O$_4$ composites were displayed in Fig. 3. In the case of PANI, only a broad band appears at a 2θ value of 25°, which is ascribed to the periodicity parallel to the polymer chains of PANI [21] and can also be found in other spectra. In Fig. 3a, b and c, the characteristic diffraction peaks of Fe$_3$O$_4$ NPs at $2\theta = 29.9°$, 35.4°, 43.1°, 57.2° and 62.8° can be observed. These data are in good agreement with that of Fe$_3$O$_4$ NPs reported before [16]. Besides the PANI and Fe$_3$O$_4$ peaks, characteristic peaks of Pd NPs at 40.1°, 46.6° and 68.1° can be observed in Fig. 3b and characteristic peaks of Au NPs at 38.18°, 44.39°, and 64.58° can be observed in Fig. 3a. The peaks of Pd NPs are assigned to (111), (110), (100) crystalline plane of Pd, respectively [22], while the peaks of Au NPs represented Bragg reflections from (111), (200), and (220) planes of Au. These data confirmed that the metal oxide and metal NPs were successfully incorporated into the PANI matrices.

The magnetic properties of obtained composites were investigated with a vibrating sample magnetometer. Typical magnetization curves as a function of applied field at room temperature (300 K) were shown in Fig. 4. There is no pronounced hysteresis loop, which indicates that both the retentivity and the coercivity of the composites are zero. This observation is consistent with superparamagnetic behavior. As shown in Fig. 4, the PANI/Fe$_3$O$_4$ composite has a saturated magnetization of $M_s = 17.85$ emu/g and the PANI/Fe$_3$O$_4$/Pd hollow spheres has a saturated magnetization of $M_s = 12.38$ emu/g. The saturated magnetization of PANI/Fe$_3$O$_4$/Au was almost same to PANI/Fe$_3$O$_4$/Pd hollow spheres, so we displayed their magnetization curves in separate patterns (left top in Fig. 4). The reason why PANI/Fe$_3$O$_4$/Pd and PANI/Fe$_3$O$_4$/Au have similar magnetizations is that the contents of Fe$_3$O$_4$ are close in the two nanocomposites. According to the ICP results, the weight percentage of Fe$_3$O$_4$ in PANI/Fe$_3$O$_4$/Pd is 45.76% while the percentage in PANI/Fe$_3$O$_4$/Au is about 42.29%.

The magnetic separability of such magnetic nanocomposites (take PANI/Fe$_3$O$_4$/Pd as an example) was tested by placing a magnet near the quartz absorption cell. As shown in Fig. 5, the black green particles were attracted toward the magnet in a very short time, demonstrating that this nanocomposite could be employed for magnetic catalyst loading which provide an easy and efficient way to separate and recycle the materials from heterogeneous reaction systems.

3.2. Electrochemical behavior of DA at the PANI/Fe$_3$O$_4$/Au-decorated GCE

DA is an important neurotransmitter in mammalian central nervous systems [23]. Changes in DA levels have proved to be important in effective brain function, for example, learning and memory formation, and in the physiological and pathological process of Parkinson's disease [24,25]. Quantitative determination of DA is therefore important and has attracted much interest of neuroscientists and chemists. Electrochemical detection is a feasible method because DA is electrochemically active and electrochemical methods have advantages such as simplicity, speed, and sensitivity. As a result, as-synthesized PANI/Fe$_3$O$_4$/Au hollow spheres have been decorated on the GCE for the detection of dopamine. Fig. 6 shows a series of CVs obtained from DA with different concentrations at the PANI/Fe$_3$O$_4$/Au-modified GCE electrode in 0.05 M PBS (pH 7.0). The oxidation peak in the presence of DA appears at 243 mV which is similar to that reported by Yin et al. [26]. It can also be seen that the oxidation peak current is increased with the gradual addition of DA, showing the catalytic property of the modified electrode in the oxidation of DA. Furthermore, the electrocatalytic anodic current in the PANI/Fe$_3$O$_4$/Au system is much higher than ever reported systems. For example, Zhu et al. reported that at a DA concentration of 10 mM, the PANI/Au system generates an
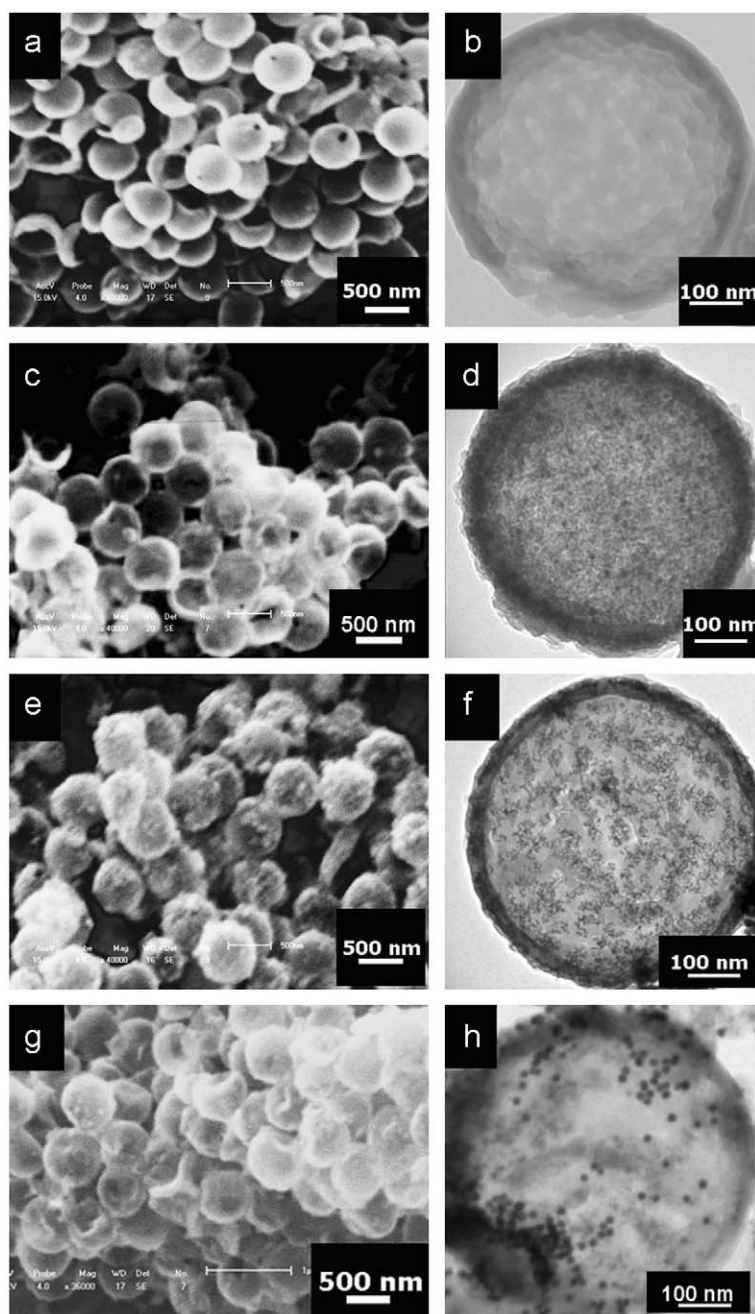
Fig. 1. SEM images of (a) PANI; (c) PANI/Fe$_3$O$_4$; (e) Au NPs/PANI/Fe$_3$O$_4$; (g) Pd NPs/PANI/Fe$_3$O$_4$ hollow spheres and TEM images of (b) PANI; (d) PANI/Fe$_3$O$_4$; (f) Au NPs/PANI/Fe$_3$O$_4$; (h) Pd NPs/PANI/Fe$_3$O$_4$ hollow spheres.

anodic current of 54.1 μA [2] while in our system, at a DA concentration of 0.9 mM, the anodic current was already 31.43 μA. The improved electrocatalytic oxidation of DA may be due to the fact that in our product, besides the facilitated electrical contacting of the redox DA with the electrode and enhanced electron transfer which is attributed to the charge hopping through the metallic conductor Au NPs and the large surface area of the hollow spheres [2], the presence of Fe$_3$O$_4$ NPs can also favor the absorption of DA. The effective transport of the electrons from DA to the electrode leads to the efficient electrocatalytic oxidation of DA.

Fig. 7 indicates that the logarithm of anodic peak current was proportional to the logarithm of DA concentration. The linear regression equation was lg[current]/

μA = 4.2488+0.89437lg[concentration]/mol L^{-1} with a correlation coefficient of $r = 0.9973$ ($n = 8$, RSD = 1.6%). As the results show, we can deduce the DA concentration from the value of anodic peak current, thus determine the DA concentration quantitatively.

### 3.3. Catalytic activity of PANI/Fe$_3$O$_4$/Pd on the reduction of 4-nitroaniline

The catalytic activity of PANI/Fe$_3$O$_4$/Pd on the reduction of 4-nitroaniline was investigated and compared to Pd/C (10%) catalyst. The reduction reaction of 4-nitroaniline by NaBH$_4$ in the absence of catalyst was quite slow and many kinds of catalysts have been
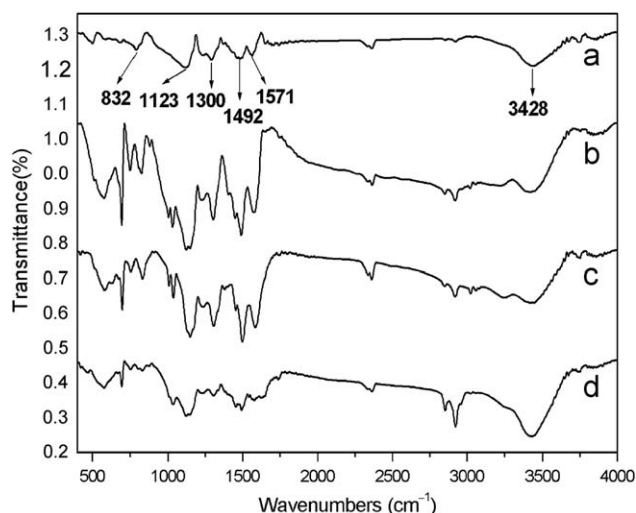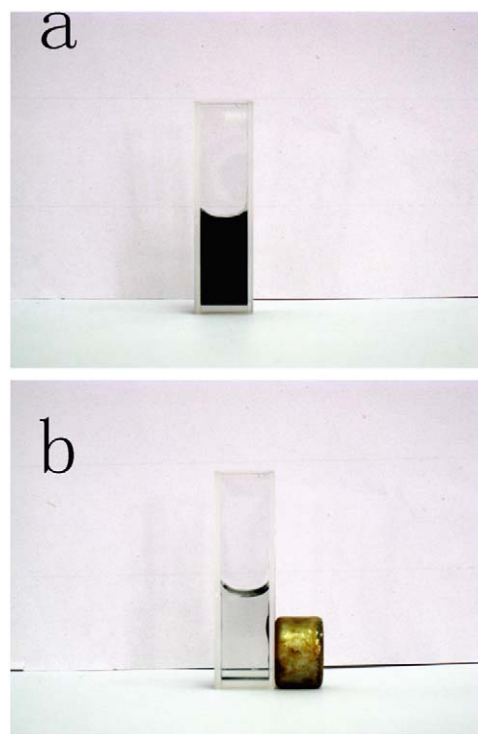
Fig. 2. IR spectrum of (a) PANI; (b) PANI/Fe$_3$O$_4$; (c) Au NPs/PANI/Fe$_3$O$_4$; and (d) Pd NPs/PANI/Fe$_3$O$_4$ hollow spheres.
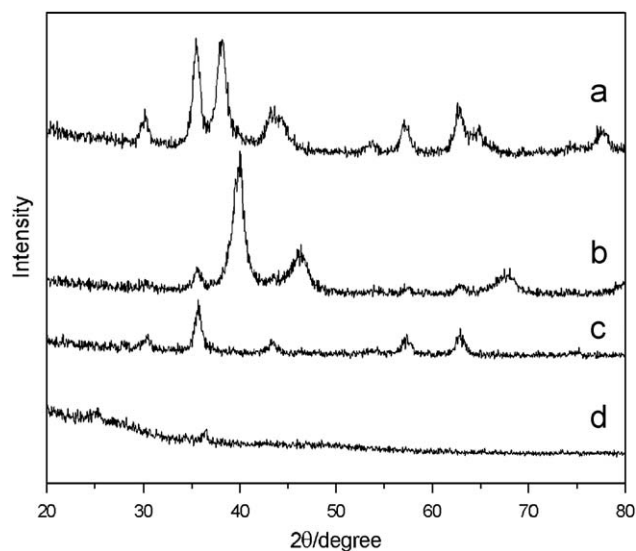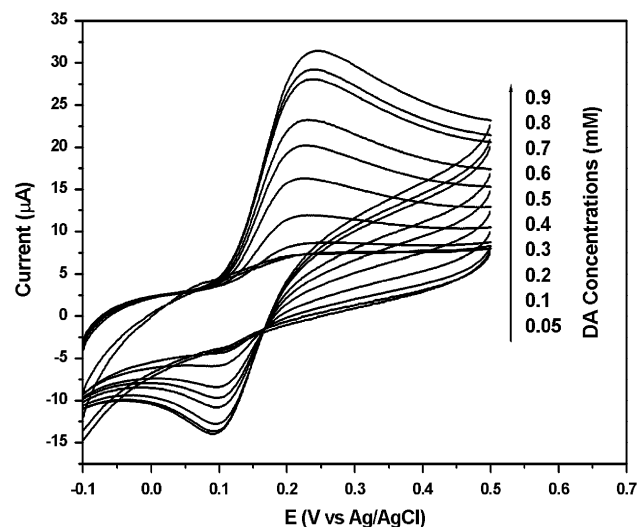

Fig. 3. XRD spectrum of (a) Au NPs/PANI/Fe$_3$O$_4$; (b) Pd NPs/PANI/Fe$_3$O$_4$; (c) PANI/Fe$_3$O$_4$ hollow spheres and (d) PANI.
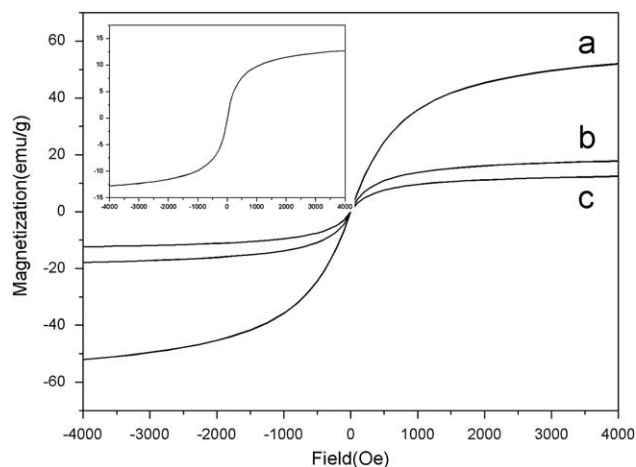
Fig. 4. Magnetization versus applied magnetic field at room temperature for (a) PANI; (b) PANI/Fe$_3$O$_4$; (c) Pd NPs/PANI/Fe$_3$O$_4$ and Au NPs/PANI/Fe$_3$O$_4$ hollow spheres (inserted).

Fig. 5. Separability of PANI/Fe$_3$O$_4$/Pd hollow spheres by placing an external magnetic field.

Fig. 6. Cyclic voltammograms of PANI/Fe$_3$O$_4$/Au-decorated GCE in the presence of different concentrations of dopamine at the scan rate 100 mV/s.

used to catalyze this reaction [27,28]. As can be seen in Fig. 8, the spectrum of the mixture of the 4-nitroaniline and NaBH$_4$ solutions is dominated by the band at 380 nm, which corresponds to intermolecular charge transfer for 4-nitroaniline. The intensity of this characteristic band decreases very few after 12 h. However, the reduction reaction of 4-nitroaniline was greatly accelerated after the addition of PANI/Fe$_3$O$_4$/Pd aqueous solution. The successive absorption spectra of the reduction of 4-nitroaniline catalyzed by PANI/Fe$_3$O$_4$/Pd and Pd/C (10%) catalyst are shown in Fig. 9. In the presence of as-synthesized product, the band at 380 nm quickly decreases and totally disappears only after 7.5 min. At the same time, a new band is developed at 240 nm,
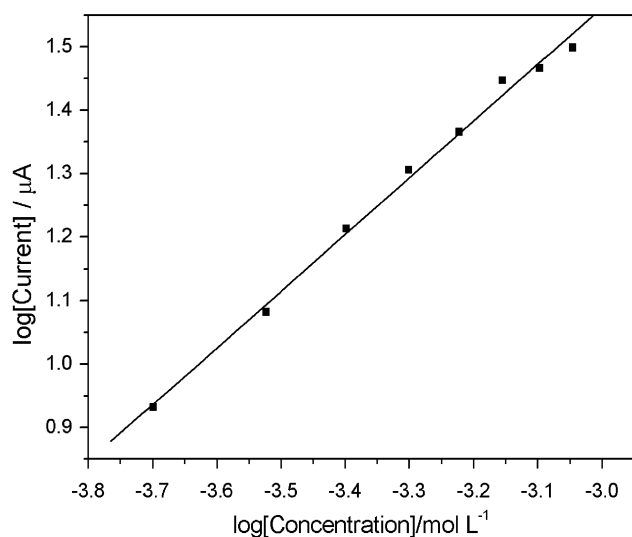
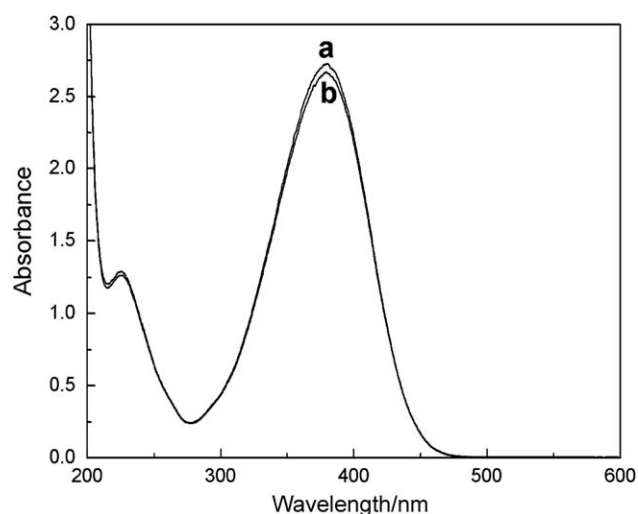**Fig. 7.** Concentration calibration plot of the anodic peak current for DA.

Fig. 8. Absorption spectra of 4-nitroaniline and borohydride mixed aqueous solution after (a) 1 min and (b) 12 h.

Fig. 9. Successive absorption spectra of aqueous solution containing 4-nitroaniline and borohydride after the addition of (a) PANI/Fe$_3$O$_4$/Pd aqueous dispersion and (b) Pd/C aqueous dispersion.

corresponding to the formation of 4-phenylenediamine in the solution, indicating the completely reduction of 4-nitroaniline. Comparatively, after the addition of Pd/C aqueous solution (the used Pd content is 0.2 mg/mL and it was kept same when using Pd/C catalyst as that when using PANI/Fe$_3$O$_4$/Pd as the catalyst), the reduction peak does not disappear even after 20 min. The results indicated that the catalytic activity of PANI/Fe$_3$O$_4$/Pd is superior to Pd/C catalyst. This may be due to the fact that in our products, Pd NPs were evenly dispersed in the PANI matrix. As a result, the catalyst has large surface areas which can offer more catalytic areas. The reductive and conductive PANI can accelerate the electron transfer from the NaBH$_4$ to PANI, then to Pd NPs and finally to 4-nitroaniline. The PANI acts as a redox mediator to help shuttle electrons between the reactants. All in all, their large surface areas and the synergistic effect between Pd NPs and their support facilitated the electron transfer between the reactants [29].

More detailed information about the catalytic activity of the composites is known by studying the kinetics of the reduction reaction. The sodium borohydride in the reactive system is requested to greatly exceed the content of 4-nitroaniline, so that
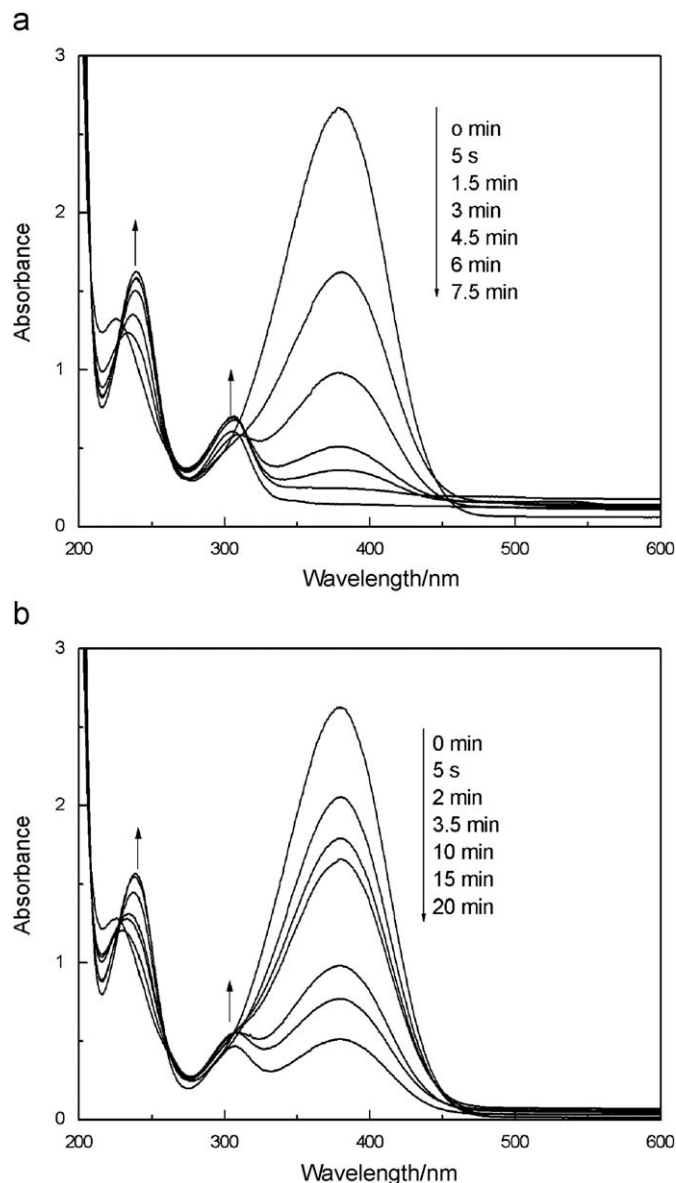
the rates of the reduction are assumed to be independent of the concentration of sodium borohydride, and thus the kinetics of the reduction could be treated as pseudo-fist-order in 4-nitroaniline concentration [30,31]. The ratio of absorbance A_t of 4-nitroaniline at time t to its value A_0 measured at $t = 0$ directly gives the corresponding concentration ratios C/C_0 of 4-nitroaniline. Thus the kinetic equation of the reduction could be shown as $dC_t/dt = K_{app}t$ or $\ln(C_0/C_t) = \ln(A_0/A_t) = K_{app}t$, where C_t is the concentration of 4-nitroaniline at time t and K_{app} is the apparent rate constant, which can be obtained from the decrease of peak intensity at 380 nm with time.

According to the above equation, the relations of $\ln(C_0/C_t)$ versus time t are obtained and shown in Fig. 10. It is clear that $\ln(C_0/C_t)$ shows linear variation with the reaction time. The value of K_{app} is obtained by calculating the slope of the fitting line and is 0.4574 to Pd/Fe$_3$O$_4$/PANI while 0.0689 to Pd/C. Higher value of K_{app} means higher catalytic activity of the catalyst. According to the results, we can calculate the approximate time to reduce a certain amount of 4-nitroaniline.
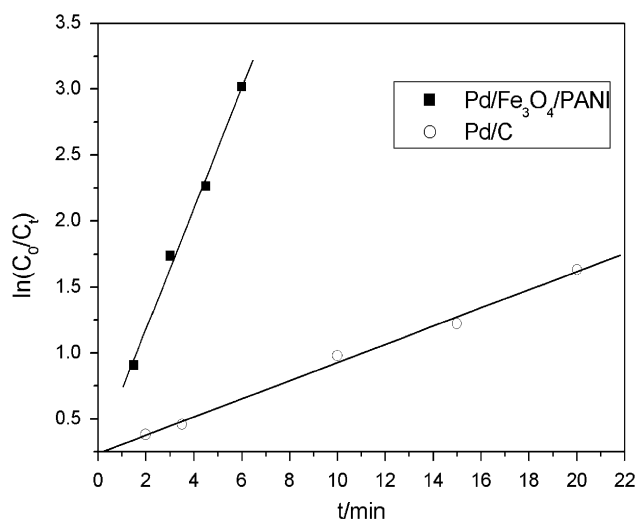
Fig. 10. The linear fit of $\ln(C_0/C_t)$ versus time using Pd/Fe$_3$O$_4$/PANI or Pd/C as the catalyst.

4. Conclusions

In conclusion, we have constructed two novel magnetic PANI/metal hybrid nanostructures using polyaniline/Fe$_3$O$_4$ composite hollow spheres as supports. In catalysis, these nanocomposites provide not only large surface areas for high loading of catalysts but also the ability to be easily separated from reaction mixture by means of the using of an external magnetic field. PANI/Fe$_3$O$_4$/Au hollow spheres have been decorated on the GCE for the detection of dopamine and PANI/Fe$_3$O$_4$/Pd hollow spheres have been used to catalyze the reduction of 4-nitroaniline. The results showed that these as-synthesized magnetic organic–inorganic composites have enhanced electrocatalytic or catalytic activities. This method could be extended to prepare other magnetic composite hollow spheres with different compositions.

References

[1] For reviews, see: (a) W. SchHrtl, Adv. Mater. 12 (2000) 1899 and references therein; (b) F. Caruso, Adv. Mater. 13 (2001) 11 and references therein.
[2] X.M. Feng, C.J. Mao, G. Yang, W.H. Hou, J.J. Zhu, Langmuir 22 (2006) 4384.
[3] M.G. Kanatzidis, C.G. Wu, H.O. Marcy, C.R. Kannewurf, J. Am. Chem. Soc. 111 (1989) 4139.
[4] C.G. Wu, D.C. DeGroot, H.O. Marcy, J.L. Schindler, C.R. Kannewurf, T. Bakas, V. Papaefthymiou, W. Hirpo, J.P. Yesinowski, M.G. Kanatzidis, J. Am. Chem. Soc. 117 (1995) 9229.
[5] L. Wang, P. Brazis, M. Rocci, C.R. Kannewurf, M.G. Kanatzidis, Chem. Mater. 10 (1998) 3298.
[6] R. Bissessur, D.C. DeGroot, J.L. Schindler, C.R. Kannewutf, M.G. Kanatzidis, J. Chem. Soc. Chem. Commun. (1993) 687.
[7] M.G. Kanatzidis, C.G. Wu, H.O. Marcy, D.C. DeGroot, C.R. Kannewurf, A. Kostikas, V. Papaefthymiou, Adv. Mater. 2 (1990) 364.
[8] B.M. Choudary, M. Roy, S. Roy, M.L. Kantam, B. Sreedhar, K.V. Kumar, Adv. Synth. Catal. 348 (2006) 1734.
[9] A. Houdayer, R. Schneider, D. Billaud, J. Ghanbaja, J. Lambert, Appl. Organomet. Chem. 19 (2005) 1239.
[10] T. Sen, A. Sebastianelli, L.J. Bruce, J. Am. Chem. Soc. 128 (2006) 7130.
[11] T.R. Sathe, A. Agrawal, S. Nie, Anal. Chem. 78 (2006) 5627.
[12] J. Kim, J. Lee, H.B. Na, B.C. Kim, J.K. Youn, J.H. Kwak, K. Moon, E. Lee, J. Kim, J. Park, A. Dohnalkova, H.G. Park, M.B. Gu, H.N. Chang, J.W. Grate, T. Hyeon, Small 1 (2005) 1203.
[13] C.S. Kumar, J. Hormes, C. Leuschner, Nanofabrication Towards Biomedical Applications, Wiley-VCH Weinheim, New York, 2005.
[14] S. Mornet, S. Vasseur, F. Grasset, E.J. Duguet, J. Mater. Chem. 14 (2004) 2161.
[15] J. Won, M. Kim, Y.W. Yi, Y.H. Kim, N. Jung, T.K. Kim, Science 309 (2005) 121.
[16] X.F. Lu, Y.H. Yu, L. Chen, H. Mao, H. Gao, J. Wang, W.J. Zhang, Y. Wei, Nanotechnology 16 (2005) 1660.
[17] X.F. Lu, H. Mao, D.M. Chao, W.J. Zhang, Y. Wei, J. Solid State Chem. 179 (2006) 2609.
[18] A. Doron, E. Katz, I. Willner, Langmuir 11 (1995) 1313.
[19] X.F. Lu, Y.H. Yu, L. Chen, H. Mao, W.J. Zhang, Y. Wei, Chem. Commun. 13 (2004) 1522.
[20] Z.J. Wang, J.H. Yuan, M.Y. Li, D.X. Han, Y.J. Zhang, Y.F. Shen, L. Niu, A. Ivaska, J. Electroanal. Chem. 599 (2007) 121.
[21] S.K. Pillalamarri, F.D. Blum, S.T. Tokuhiro, J.G. Storyand, M.F. Bertino, Chem. Mater. 17 (2005) 227.
[22] G. Chang, M. Oyamaand, K. Hirao, J. Phys. Chem. B 110 (2006) 20362.
[23] R. Wightman, C. Amatorh, R. Engstrom, P. Hale, E. Kristensen, W. Kubr, L. May, Neuroscience 25 (1988) 513.
[24] R. Wightman, L. May, A. Michael, Anal. Chem. 60 (1988) 769A.
[25] R. Adams, Anal. Chem. 48 (1976) 1128A.
[26] T.J. Yin, W.Z. Wei, J.X. Zeng, Anal. Bioanal. Chem. 386 (2006) 2087.
[27] Q. Zhou, G.Z. Qian, Y. Li, G. Zhao, Y.W. Chao, J.W. Zheng, Thin Solid Films 516 (2008) 953.
[28] T. Vincent, F. Peirano, E. Guibal, J. Appl. Polym. Sci. 94 (2004) 1634.
[29] B.J. Gallon, R.W. Kojima, R.B. Kanerand, P.L. Diaconescu, Angew. Chem. Int. Ed. 46 (2007) 7251.
[30] Y. Mei, Y. Lu, F. Polzer, M. Ballauff, M. Drechsler, Chem. Mater. 19 (2007) 1062.
[31] Y. Wang, G. Wei, W. Zhang, X. Jiang, P. Zheng, L. Shi, A. Dong, J. Mol. Catal. A 266 (2007) 233.